

Pentamethylcyclopentadienyllgallium (Cp*Ga): Alternative Synthesis and Application as a Terminal and Bridging Ligand in the Chemistry of Chromium, Iron, Cobalt, and Nickel†

Peter Jutzi,* Beate Neumann, Guido Reumann, and Hans-Georg Stammler

Fakultät für Chemie, Universität Bielefeld, Bielefeld, Germany

Received October 20, 1997

An alternative synthetic route to η^5 -pentamethylcyclopentadienyllgallium ($\text{Me}_5\text{C}_5\text{Ga}$, Cp*Ga, **1**) via reductive dehalogenation of (pentamethylcyclopentadienyl)diiodogallane (Cp^*GaI_2 , **2**) is reported. In addition, the behavior of compound **1** as a ligand in transition metal chemistry is examined. In the reaction of **1** with $\text{Cr}(\text{CO})_5(\text{C}_8\text{H}_{14})$ ($\text{C}_8\text{H}_{14} = \text{cis-cyclooctene}$), $\text{Fe}_2(\text{CO})_9$, $\text{Fe}(\text{CO})_3\text{CHT}$ (CHT = cycloheptatriene), $\text{Co}_2(\text{CO})_8$, and $\text{Ni}(\text{CO})_4$ the new complexes $\text{Cr}(\text{Cp}^*\text{Ga})(\text{CO})_5$ (**3**), $\text{Fe}(\text{Cp}^*\text{Ga})(\text{CO})_4$ (**4**), $\text{Fe}_2(\mu\text{-Cp}^*\text{Ga})_3(\text{CO})_6$ (**5**), $\text{Co}_2(\mu\text{-Cp}^*\text{Ga})_2(\text{CO})_6$ (**6**), and $\text{Ni}_4(\mu\text{-Cp}^*\text{Ga})_4(\text{CO})_6$ (**8**), respectively, were obtained. They were characterized by analytical and spectroscopic methods; solid-state structures were determined by X-ray diffraction analysis. In the reaction of **1** with $\text{Ni}(\text{CO})_4$, the complex $\text{Ni}(\text{Cp}^*\text{Ga})(\text{CO})_3$ (**7**) is an intermediate, which was characterized by IR and NMR data. The η^5 -bonding mode within the Cp*Ga ligand is maintained, apart from one Cp*Ga unit in **5** which exhibits η^3/η^1 -bonding. The cone angle of $\eta^5\text{-Cp}^*\text{Ga}$ is 112° , as determined on the basis of structural data of **3** and **4**. Concerning the σ -donor/ π -acceptor properties, **1** is classified as a predominant electron donor.

Introduction

In the last few years, the inorganic and organometallic chemistry of monovalent gallium has attracted much attention; several compounds have been synthesized and characterized only recently.^{1,2} Pentamethylcyclopentadienyllgallium ($\text{Me}_5\text{C}_5\text{Ga}$, Cp*Ga, **1**) was first prepared by Schnöckel et al. using metastable solutions of $\text{Ga}(\text{I})\text{Cl}$, which are difficult to prepare.^{1c} These solutions react with Cp^*_2Mg or Cp^*Li to give Cp*Ga in unspecified yields.^{2b} The fundamental properties of Cp*Ga have been described by Schnöckel et al. Interestingly, Cp*Ga is a monomer in the gas phase and in solution but forms a hexamer in the solid state.^{3,4}

A common synthetic route to sandwich or half-sandwich complexes of subvalent main group elements is the reductive dehalogenation of Cp^*_nMX_m compounds. As an impressive example, decamethylsilicocene (Cp^*_2 -

Si) can be obtained in good yield by reduction of $\text{Cp}^*_2\text{-SiCl}_2$ with alkali metal naphthalenides.⁵ As an example from group 13 chemistry, the cluster compound $(\text{Cp}^*\text{Al})_4$, which was first synthesized by Schnöckel et al.,⁶ can also be obtained by reduction of Cp^*AlCl_2 with potassium in 20% yield.⁷ We report here a procedure to prepare Cp*Ga in good yield via reductive dehalogenation of Cp^*GaI_2 with potassium using ultrasonic metal activation.

Due to the metal-centered lone pair, monovalent group 13 compounds principally act as donor ligands in transition metal chemistry, as exemplified by species such as $\text{Me}_5\text{C}_5\text{Al}$ (Cp^*Al)⁸ and $\text{InC}(\text{SiMe}_3)_3$.⁹ As part of our studies concerning the reactivity of Cp*Ga, we report the synthesis and structural characterization of the coordination compounds $\text{Cr}(\text{Cp}^*\text{Ga})(\text{CO})_5$, **3**, $\text{Fe}(\text{Cp}^*\text{Ga})(\text{CO})_4$, **4**, $\text{Fe}_2(\text{Cp}^*\text{Ga})_3(\text{CO})_6$, **5**, $\text{Co}_2(\text{Cp}^*\text{Ga})_2(\text{CO})_6$, **6**, and $\text{Ni}_4(\text{Cp}^*\text{Ga})_4(\text{CO})_6$, **8**, in which Cp*Ga for the first time acts as a donor ligand in transition metal chemistry.

* Prof. Dr. Peter Jutzi, Fakultät für Chemie, Universität Bielefeld, Universitätsstrasse, 33615 Bielefeld.

† Dedicated to Prof. Achim Müller on the occasion of his 60th birthday.

(1) Schmidbaur, H. *Angew. Chem.* **1985**, *97*, 893; *Angew. Chem., Int. Ed. Engl.* **1985**, *24*, 893. (b) Dohmeier, C.; Loos, D.; Schnöckel, H. *Angew. Chem.* **1996**, *108*, 141; *Angew. Chem., Int. Ed. Engl.* **1996**, *35*, 129. (c) Tacke, M.; Plaggenborg, L.; Schnöckel, H. *Z. Anorg. Allg. Chem.* **1991**, *604*, 35.

(2) Kuchta, M. C.; Bonanno, J. B.; Parkin, G. *J. Am. Chem. Soc.* **1996**, *118*, 10914. (b) Loos, D.; Schnöckel, H. *J. Organomet. Chem.* **1993**, *463*, 37. (c) Uhl, W.; Hiller, W.; Layh, M.; Schwarz, W. *Angew. Chem.* **1992**, *104*, 1378; *Angew. Chem., Int. Ed. Engl.* **1992**, *31*, 1364. (d) Linti, G. *J. Organomet. Chem.* **1996**, *520*, 107. (e) Beachley, O. T., Jr.; Patzik, J.; Noble, M. J. *Organometallics* **1994**, *13*, 2885.

(3) Loos, D.; Baum, E.; Ecker, A.; Schnöckel, H.; Downs, A. J. *Angew. Chem.* **1997**, *109*, 894; *Angew. Chem., Int. Ed. Engl.* **1997**, *36*, 860.

(4) Haaland, A.; Martinsen, K. G.; Volden, H. V.; Loos, D.; Schnöckel, H. *Acta Chem. Scand.* **1994**, *48*, 172.

(5) Jutzi, P.; Kanne, D.; Krüger, C. *Angew. Chem.* **1986**, *98*, 163; *Angew. Chem., Int. Ed. Engl.* **1986**, *25*, 164.

(6) Dohmeier, C.; Robl, C.; Tacke, M.; Schnöckel, H. *Angew. Chem.* **1991**, *103*, 594; *Angew. Chem., Int. Ed. Engl.* **1991**, *30*, 564.

(7) Schulz, S.; Roesky, H. W.; Koch, H. J.; Sheldrick, G. M.; Stalke, D.; Kuhn, A. *Angew. Chem.* **1993**, *105*, 1828; *Angew. Chem., Int. Ed. Engl.* **1993**, *32*, 1729.

(8) Dohmeier, C.; Krautscheid, H.; Schnöckel, H. *Angew. Chem.* **1994**, *106*, 2570; *Angew. Chem., Int. Ed. Engl.* **1994**, *33*, 2482. (b) Weiss, J.; Stetzkamp, D.; Nuber, B.; Fischer, R. A.; Boehme, C.; Frenking, G. *Angew. Chem.* **1997**, *109*, 95; *Angew. Chem., Int. Ed. Engl.* **1997**, *36*, 70.

(9) Uhl, W.; Pohlmann, M. *Organometallics* **1997**, *16*, 2478. (b) Uhl, W.; S. U. Keimling, Hiller, W.; Neumayer, M. *Chem. Ber.* **1996**, *129*, 397. (c) Uhl, W.; Keimling, S. U.; Hiller, W.; Neumayer, M. *Chem. Ber.* **1995**, *128*, 1137.

Scheme 1

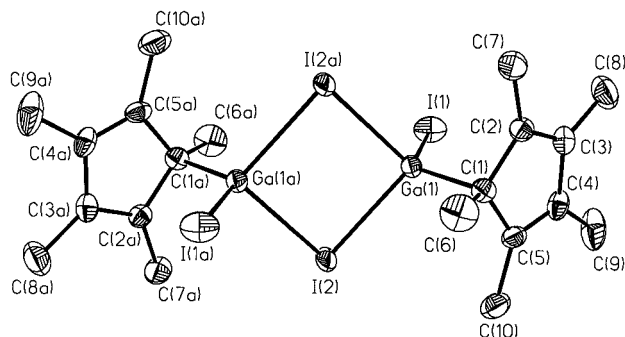
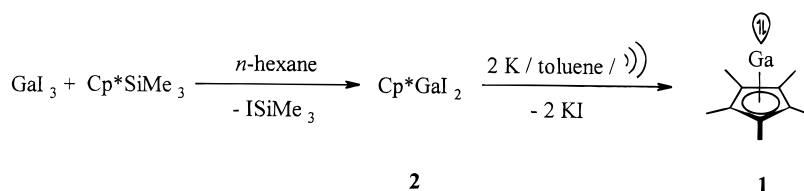
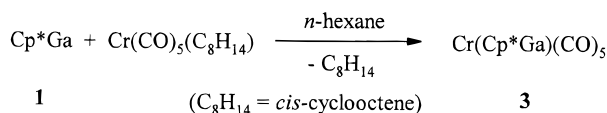


Figure 1. Molecular structure of Cp^*GaI_2 , **2**.

Scheme 2



Results and Discussion

Pentamethylcyclopentadienylgallium dihalides can be regarded as useful starting materials for the synthesis of Cp^*Ga (**1**) by reductive dehalogenation. Keeping in mind the leaving group character of cyclopentadienyl ligands and the competition in elimination reactions,¹⁰ the diiodo compound Cp^*GaI_2 (**2**) seems to be the most suitable for a successful reduction process.

Compound **2** was prepared by the reaction of Cp^*SiMe_3 ¹¹ with GaI_3 in refluxing *n*-hexane (see Scheme 1). After evaporation the solvent and of Me_3SiI , **2** could be obtained in very high yield following crystallization from a *n*-hexane/toluene mixture as an orange air- and moisture-sensitive compound. As shown by an X-ray structure analysis, **2** exists as an iodo-bridged dimer with σ -bonded Cp^* ligands. There are no extraordinary structural features compared to the corresponding chloro compound Cp^*GaCl_2 ,¹² so the structure is not discussed in detail here. The molecular structure of **1** is shown in Figure 1. Crystallographic data are given in Table 1, and selected bond lengths and angles are collected in Table 2.

For the synthesis of **1**, a solution of **2** in toluene was treated with a small excess of potassium under ultrasonic activation at 70 °C (see Scheme 2). After filtration and evaporation of the solvent, compound **1** was obtained in good yield by distillation in vacuo as a slightly yellow, air-sensitive liquid, which solidified after several days during storage at 4 °C. The spectroscopic data (¹H and ¹³C NMR) agree well with those reported by Schnöckel et al.^{2b}

The exceptional thermal stability of **1** is worth mentioning. Fractional distillation at 80 °C could be performed without any decomposition. Furthermore, under MOMBE (metal organic molecular beam epitaxy) conditions, **1** turned out to be stable toward fragmentation up to temperatures of approximately 600 °C.¹³

Recent investigations show that **1** can also be prepared starting from the dichloro (Cp^*GaCl_2) or the dibromo (Cp^*GaBr_2) compound, but in somewhat lower yields. In the reaction with Cp^*GaCl_2 , the compound $\text{K}[\text{Cp}^*\text{GaCl}_3]$ is an intermediate; it forms a tetrameric aggregate in the solid state.¹⁴

Due to the fact that **1** possesses a nonbonding electron pair (lone pair), Lewis-base activity can be anticipated. Thus, **1** should act as a σ -donor ligand in transition metal chemistry. Keeping in mind the easy haptotropic shift in main group cyclopentadienyl compounds,¹⁵ an $\eta^5 \rightarrow \eta^3 \rightarrow \eta^1$ rearrangement in **1** might create vacant coordination sites at the gallium center. As a result, **1** might act also as a π -acceptor ligand. In this context, the application of **1** as a ligand in transition metal complexes is of special interest. We started our investigations with examples from the chemistry of chromium, iron, cobalt, and nickel.

When a solution of $\text{Cr}(\text{CO})_5(\text{C}_8\text{H}_{14})$ (C_8H_{14} = *cis*-cyclooctene)¹⁶ and **1** in *n*-hexane was heated under reflux, the cyclooctene ligand was replaced by **1** and the complex $\text{Cr}(\text{Cp}^*\text{Ga})(\text{CO})_5$, **3**, was formed (see Scheme 2). Removal of all volatile components in vacuo led to an air-sensitive yellow powder which was recrystallized from hot *n*-hexane for further purification. Compound **3** exhibits a sharp melting point at 156 °C and decomposes at approximately 240 °C. The complex dissolves easily in aprotic organic solvents. Crystals suitable for an X-ray structure analysis were obtained from a *n*-hexane solution. The molecular structure of **3** is shown in Figure 2. Crystallographic data are given in Table 1, and selected bond lengths and angles are collected in Table 3.

In compound **3**, the chromium atom is positioned in an octahedral coordination sphere. Cp^*Ga is a terminal ligand with a Cr–Ga distance of 2.4046(7) Å. The small deviation of the Cp(centroid)–Ga–Cr vector from linearity presumably is caused by packing effects. Within the Cp^*Ga fragment, the η^5 -bonding mode of the Cp^* ring is maintained; the Ga–C distances are quite similar, with an average value of 2.260(3) Å. Compound **3** exhibits Cr–C(CO) distances in the normal range observed for $\text{Cr}(\text{CO})_5\text{L}$ complexes. Thus, all equatorial Cr–C(CO) distances are equal within experimental

(10) Jutzi, P.; *Comm. Inorg. Chem.* **1987**, *6*, 123.

(11) Llinas, G. H.; Mena, M.; Palacios, F.; Royo, P.; Serrano, R. *J. Organomet. Chem.* **1988**, *340*, 37.

(12) Beachley, O. T.; Hallock, R. B.; Zhang, H. M.; Atwood, J. L. *Organometallics* **1985**, *4*, 1675.

(13) Aschentrup, A.; Moltchanov, A.; Tappe, T.; Schmiedeskamp, B.; Reumann, G.; Jutzi, P. Manuscript in preparation.

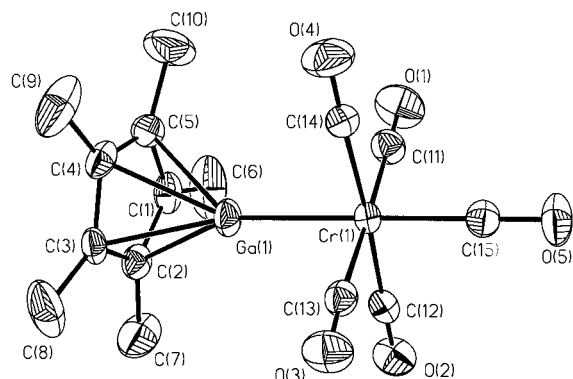
(14) Jutzi, P.; Reumann, G. Manuscript in preparation.

(15) Fisher, J. D.; Budzelaar, P. H. M.; Shapiro, P. J.; Staples, R. J.; Yap, G. P. A.; Rheingold, A. L. *Organometallics* **1997**, *16*, 871.

(16) Grevels, F. W.; Skibbe, V. *J. Chem. Soc., Chem. Commun.* **1984**, 681.

Table 1. Crystallographic Data for 2, 3, 4, 5, 6, and 8

	C ₁₀ H ₁₅ Gal ₂ , 2	C ₁₅ H ₁₅ CrGaO ₃ , 3	C ₁₄ H ₁₅ FeGaO ₄ , 4	C ₃₀ H ₄₅ Fe ₂ Ga ₃ O ₆ , 5	C ₂₀ H ₃₀ Co ₂ Ga ₂ O ₆ , 6	C ₄₀ H ₆₀ Ga ₄ Ni ₄ O ₆ ·2C ₇ H ₈ , 8
empirical formula	C ₁₀ H ₁₅ Gal ₂ , 2	C ₁₅ H ₁₅ CrGaO ₃ , 3	C ₁₄ H ₁₅ FeGaO ₄ , 4	C ₃₀ H ₄₅ Fe ₂ Ga ₃ O ₆ , 5	C ₂₀ H ₃₀ Co ₂ Ga ₂ O ₆ , 6	C ₄₀ H ₆₀ Ga ₄ Ni ₄ O ₆ ·2C ₇ H ₈ , 8
fw	458.74	396.99	372.83	894.58	695.80	1406.93
cryst color, habit	orange, irregular	yellow, cube	yellow, irregular	red, irregular	red-brown, needles	red, plates
cryst size, mm ³	1.00 × 0.80 × 0.60	0.30 × 0.20 × 0.20	0.1 × 0.25 × 0.3	0.80 × 0.30 × 0.20	0.10 × 0.15 × 0.30	1.00 × 0.50 × 0.20
temp, K	173(2)	173(2)	183(2)	173(2)	173(2)	173(2)
wavelength			Mo Kα 0.710 73 Å (graphite monochromator)			
space group	P2 ₁ /n	Pī	Pnmm	P2 ₁ /m	P2 ₁ /c	Pī
unit cell dimens	a = 8.842(3) Å b = 15.107(4) Å c = 10.570(3) Å α = 90° β = 106.42(2)° γ = 90°	a = 8.9590(10) Å b = 9.5050(10) Å c = 10.8630(10) Å α = 72.770(10)° β = 89.300(10)° γ = 74.760(10)°	a = 14.1387(7) Å b = 9.9436(5) Å c = 11.2368(6) Å α = 90° β = 90° γ = 90°	a = 8.57(2) Å b = 19.03(2) Å c = 11.81(2) Å α = 90° β = 107.40(14)° γ = 90°	a = 17.5447(10) Å b = 8.9184(5) Å c = 17.5617(10) Å α = 90° β = 93.9030(10)° γ = 90°	a = 10.910(4) Å b = 13.263(4) Å c = 21.450(6) Å α = 103.92(2)° β = 91.13(3)° γ = 98.49(3)°
V, Å ³	1354.3(7)	850.29(15)	1479.78(14)	1837(6)	2741.5(3)	2975(2)
Z	4	2	4	2	4	2
density (calcd), Mg/m ³	2.250	1.551	1.568	1.617	1.686	1.571
θ range for data collection	2.42–32.50°	1.97–30.00°	2.32–27.15°	1.81–28.51°	3.18–27.11°	1.60–28.50°
reflections collected	5130	5261	13 830	5086	23 851	15 850
independent reflections	4867 (R _{int} = 0.0324)	4965 (R _{int} = 0.0373)	1836 (R _{int} = 0.0253)	4789 (R _{int} = 0.0436)	5892 (R _{int} = 0.0424)	15 079 (R _{int} = 0.0461)
absorption correction	semiempirical from ψ-scans	semiempirical from ψ-scans	semiempirical from equivalents	semiempirical from ψ-scans	semiempirical from equivalents	semiempirical from ψ-scans
final R indices [I > 2σ(I)]	R _F = 0.0594, R _{F²} = 0.1469	R _F = 0.0523, R _{F²} = 0.1113	R _F = 0.0223, R _{F²} = 0.0525	R _F = 0.0540, R _{F²} = 0.1062	R _F = 0.0423, R _{F²} = 0.0670	R _F = 0.0596, R _{F²} = 0.1176
no. of reflns used	3875	3388	1672	3977	4931	9979
params	123	204	134	317	335	689
largest diff. peak and hole, e Å ⁻³	1.9 and -2.3	0.456 and -0.753	0.225 and -0.469	0.7 and -0.7	0.385 and -0.360	0.8 and -0.9
diffractometer used	Siemens P2(1) diffractometer	Siemens P2(1) diffractometer	Siemens SMART CCD	Siemens P2(1) diffractometer	Siemens SMART CCD	Siemens P2(1) diffractometer
programs used						
structure refinement		Siemens SHELXTL plus/SHELXL-93 full-matrix least-squares on F ²				

**Figure 2.** Molecular structure of Cr(Cp*Ga)(CO)₅, **3**.**Table 2. Selected Bond Lengths (Å) and Angles (deg) for 2**

Ga(1)–C(1)	2.008(6)	C(1)–C(2)	1.475(9)
Ga(1)–I(1)	2.4895(11)	C(2)–C(3)	1.370(9)
Ga(1)–I(2)	2.7150(11)	C(3)–C(4)	1.451(10)
Ga(1)–I(2a)	2.7131(10)	C(4)–C(5)	1.352(10)
		C(5)–C(1)	1.491(9)
C(1)–Ga(1)–I(1)	123.6(2)	Ga(1)–C(1)–C(2)	96.5(4)
C(1)–Ga(1)–I(2)	111.5(2)	Ga(1)–C(1)–C(5)	95.7(4)
C(1)–Ga(1)–I(2a)	110.8(2)	Ga(1)–C(1)–C(6)	112.8(5)
I(2)–Ga(1)–I(2a)	92.78(2)	C(2)–C(1)–C(5)	104.9(5)

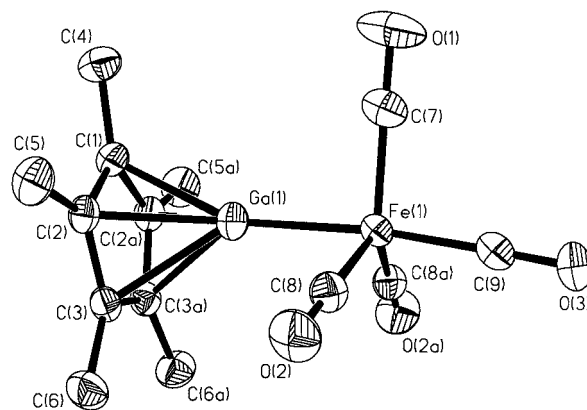
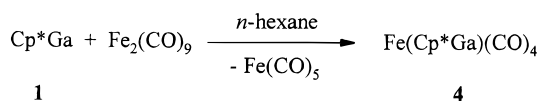
Table 3. Selected Bond Lengths (Å) and Angles (deg) for 3

Ga(1)–C(1)	2.277(3)	Cr(1)–C(11)	1.896(4)
Ga(1)–C(2)	2.246(3)	Cr(1)–C(12)	1.900(4)
Ga(1)–C(3)	2.236(3)	Cr(1)–C(13)	1.904(4)
Ga(1)–C(4)	2.260(3)	Cr(1)–C(14)	1.899(4)
Ga(1)–C(5)	2.282(4)	Cr(1)–C(15)	1.858(4)
Ga(1)–Cr(1)	2.4046(7)	O(1)–C(11)	1.143(5)
		O(2)–C(12)	1.149(5)
		O(3)–C(13)	1.142(4)
		O(4)–C(14)	1.141(4)
		O(5)–C(15)	1.146(4)

C(14)–Cr(1)–C(12)	176.62(15)	C(15)–Cr(1)–Ga(1)	179.81(12)
C(11)–Cr(1)–C(13)	178.53(15)		

error (average value 1.900(4) Å). This value is almost the same as that observed in Cr(CO)₆ (1.909(3) Å)¹⁷ or in related phosane Cr(CO)₅L complexes (e.g., 1.893 Å for L = PMe₃,¹⁸ 1.880 Å for L = PPh₃¹⁹). In contrast to the equatorial CO ligands, the axial one is more effected by the trans-orientated Cp*Ga ligand. Thus, a significantly shorter Cr–CO (trans) distance (1.858(4) Å) than in Cr(CO)₆ (1.909(3) Å) is observed, indicating a more effective electron donation from the chromium atom. The Cr–CO (trans) distance in **3** is comparable to those in Cr(CO)₅L complexes with L = PMe₃ (1.850(2) Å)¹⁸ and PPh₃ (1.845(4) Å),¹⁹ indicating similar σ-donor properties of the ligands L.

The solution-NMR data of compound **3** are in accord with the solid-state structure and with a η⁵-bonded Cp* ring. Thus, only one singlet at 1.64 ppm is observed in the ¹H NMR spectrum. Correspondingly, the ¹³C NMR spectrum shows two resonances for the Cp* ring carbon atoms (8.84 (Cp*–Me), 115.20 ppm (Cp*–ring)) and, in addition, two signals for the five carbonyl C atoms (219.01 (equatorial CO), 224.26 ppm (axial CO)). In the IR spectrum of **3**, the four absorptions observed in the

**Figure 3.** Molecular structure of Fe(Cp*Ga)(CO)₄, **4**.**Scheme 3****Table 4. Selected Bond Lengths (Å) and Angles (deg) for 4**

Ga(1)–C(1)	2.193(2)	Fe(1)–C(7)	1.789(3)
Ga(1)–C(2)	2.2110(14)	Fe(1)–C(8)	1.7885(17)
Ga(1)–C(3)	2.2576(15)	Fe(1)–C(9)	1.781(2)
Ga(1)–Fe(1)	2.2731(4)	O(1)–C(7)	1.142(3)
		O(2)–C(8)	1.147(2)
		O(3)–C(9)	1.143(3)
C(7)–Fe(1)–C(8)	118.15(5)	C(8)–Fe(1)–Ga(1)	84.01(5)
C(7)–Fe(1)–Ga(1)	90.40(9)	C(9)–Fe(1)–Ga(1)	174.34(7)

carbonyl region (2052, 1982, 1918, and 1902 cm⁻¹) are expected on the basis of a local C_{4v} symmetry; the usually IR-forbidden B₁ mode at 1982.3 cm⁻¹ is present due to the symmetry reduction caused by the C₅ symmetry of the Cp* ring. Owing to its thermal stability, compound **3** could be characterized with standard EI-MS techniques. The molecular ion is observed at 396 amu with the correct isotopic pattern; the loss of five CO molecules leads to the Cp*GaCr⁺ fragment at 256 amu with the highest observed intensity.

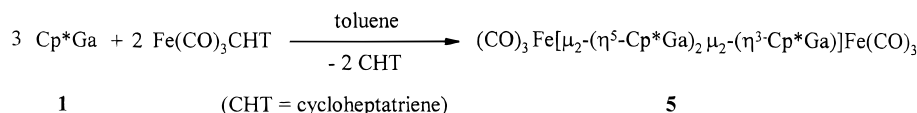
A comparable iron complex with a terminal Cp*Ga ligand was prepared using Fe₂(CO)₉ as the starting material. Thus, reaction of Fe₂(CO)₉ with **1** in *n*-hexane furnished the complex Fe(Cp*Ga)(CO)₄, **4**, in moderate yield (see Scheme 3).

Compound **4** could be isolated in pure form only by repeated recrystallization from *n*-hexane. It is an air-sensitive, yellow solid, which melts at 112 °C with decomposition accompanied by gas evolution and a color change to deep red. Dissolved in organic media, **4** decomposes very readily and, thus, must be handled with great care. Crystals suitable for an X-ray structure analysis were obtained from a *n*-hexane solution. The molecular structure of compound **4** is depicted in Figure 3. Crystal structure parameters are given in Table 1, and selected bond lengths and angles are collected in Table 4.

In compound **4**, the iron atom is surrounded by four CO ligands and one Cp*Ga ligand in a trigonal-bipyramidal geometry. The Cp*Ga ligand is fixed terminally in an axial position with an Fe–Ga distance of 2.2731(4) Å. The small deviation of the Cp*(centroid)–

(17) Whitaker, A.; Jeffery, J. W. *Acta Crystallogr.* **1967**, *23*, 977.(18) Lee, K. J.; Brown, T. L. *Inorg. Chem.* **1992**, *31*, 289.(19) Plastas, H. J.; Stewart, J. M.; Grim, S. O. *Inorg. Chem.* **1973**, *12*, 265.

Scheme 4



Ga–Fe–C(9) vector from linearity is presumably caused by packing effects. The molecule is located on a crystallographic mirror plane which is identical with the Fe–Ga–C(7) plane. Within the Cp*Ga fragment, the η^5 -bonding mode of the Cp* ring is maintained; the Ga–C distances are quite similar with an average value of 2.226(2) Å. The geometry around the iron center does not exactly correspond to a trigonal bipyramid. Thus, small deviations from the ideal angles are observed (see Table 4). All equatorial Fe–C (CO) distances are equal within the experimental error (average value 1.789(3) Å). This value is slightly smaller than that observed in Fe(CO)₅ (1.803(2) Å)²⁰ and comparable to those in related phosane Fe(CO)₄L complexes (e.g., mean value for L = P^tBu₃ is 1.792 Å,²¹ for L = PPh₃ is 1.795 Å²²). In contrast to the equatorial CO ligands, the axial one is more effected by the trans-orientated Cp*Ga ligand. Thus, a significantly shorter axial Fe–CO distance (1.781(2) Å) than in Fe(CO)₅ (1.811(2) Å)²⁰ is observed, indicating a more effective electron donation from the iron atom. The axial Fe–CO distance in **3** is comparable to those in Fe(CO)₄L complexes with P^tBu₃ (1.768(4) Å)²¹ and L = PPh₃ (1.795(4) Å),²² indicating similar σ -donor properties of the ligands L.

The η^5 -bonded Cp* ring present in the solid state is also found in solution. Thus, only one singlet at 1.60 ppm is observed in the ¹H NMR spectrum. Correspondingly, the ¹³C NMR spectrum shows two resonances for the Cp* ring (8.77 (Cp*–Me), 115.43 ppm (Cp*–ring)). In addition, only one resonance for the four carbonyl ligands is observed at 214.21 ppm, indicating pseudorotation in solution. The IR spectrum of compound **4** shows three absorptions in the carbonyl region, as expected on the basis of local C_{3v} symmetry (2037, 1966, 1942 cm⁻¹). Compound **4** could be characterized with standard EI-MS techniques. The molecular ion is observed at 372 amu with the correct isotopic pattern. The successive loss of the four CO ligands leads to the Cp*GaFe⁺ fragment at 260 amu with the highest observed intensity.

Refluxing a solution of **1** and Fe(CO)₃CHT (CHT = cycloheptatriene) in toluene led to the formation of the dinuclear iron complex (CO)₃Fe{[μ -Ga(η^5 -Cp*)]₂[μ -Ga(η^3 -Cp*)]}Fe(CO)₃ (**5**) (see Scheme 4), which could be obtained as an air-sensitive red powder after removing all volatiles in vacuo. Compound **5** dissolves easily in aprotic aromatic solvents such as toluene or benzene. In the solid-state, the complex decomposes at 270 °C. Crystals suitable for an X-ray crystal structure analysis were obtained by crystallization from hot benzene. The molecular structure of **5** is shown in Figure 4. Crystallographic data are given in Table 1, and selected bond lengths and angles are collected in Table 5.

Compound **5** can be regarded as a derivative of the dinuclear iron carbonyl complex Fe₂(CO)₉, in which the

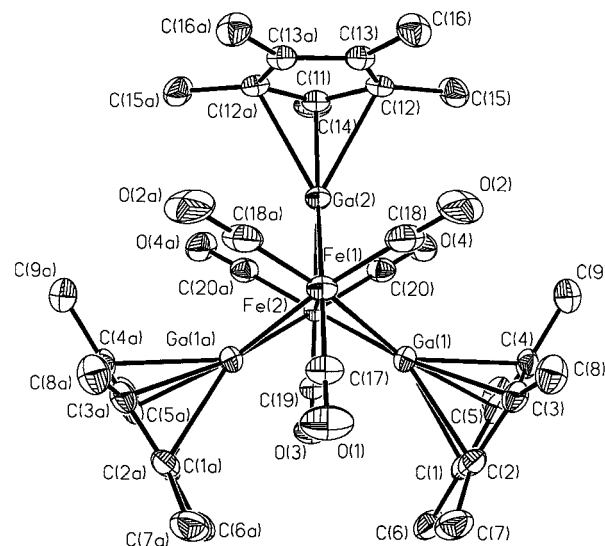


Figure 4. Molecular structure of (CO)₃Fe[μ_2 -(η^5 -Cp*Ga)₂ μ_2 -(η^3 -Cp*Ga)]Fe(CO)₃, **5**.

Table 5. Selected Bond Lengths (Å) and Angles (deg) for **5**

Ga(1)–C(1)	2.482(6)	C(1)–C(5)	1.405(7)
Ga(1)–C(2)	2.286(5)	C(1)–C(2)	1.420(7)
Ga(1)–C(3)	2.209(5)	C(2)–C(3)	1.439(7)
Ga(1)–C(4)	2.334(5)	C(3)–C(4)	1.442(6)
Ga(1)–C(5)	2.513(5)	C(4)–C(5)	1.423(7)
Ga(1)–Fe(1)	2.454(3)	Ga(2)–C(11)	2.087(7)
Ga(1)–Fe(2)	2.401(3)	Ga(2)–C(12)	2.383(5)
Ga(2)–Fe(1)	2.354(4)	Ga(2)···C(13)	2.811(5)
Ga(2)–Fe(2)	2.436(5)	C(11)–C(12)	1.448(5)
Fe(1)–Fe(2)	2.908(6)	C(12)–C(13)	1.406(6)
O(1)–C(17)	1.159(8)	C(13)–C(13a)	1.407(9)
O(2)–C(18)	1.152(6)	Fe(1)–C(17)	1.772(7)
O(3)–C(19)	1.146(8)	Fe(1)–C(18)	1.780(6)
O(4)–C(20)	1.161(5)	Fe(2)–C(19)	1.780(7)
		Fe(2)–C(20)	1.777(5)
Fe(2)–Ga(1)–Fe(1)	73.57(13)	C(20a)–Fe(2)–C(20)	99.7(3)
Fe(1)–Ga(2)–Fe(2)	74.7(2)	C(20)–Fe(2)–C(19)	98.8(2)
Ga(1)–Fe(2)–Fe(1)	54.05(9)	C(17)–Fe(1)–C(18)	98.5(2)
Ga(2)–Fe(1)–Fe(2)	53.91(13)	C(17)–Fe(1)–Fe(2)	119.8(2)
Ga(1)–Fe(1)–Fe(2)	52.38(9)	C(18)–Fe(1)–Fe(2)	116.5(2)
		C(20)–Fe(2)–Fe(1)	113.7(2)

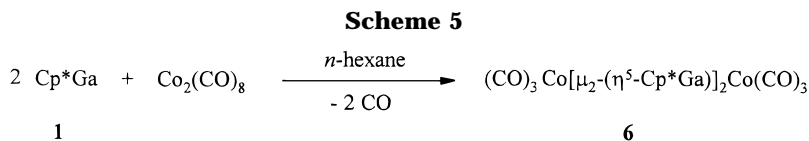
bridging carbonyl ligands are replaced by bridging Cp*Ga units resulting in D_{3h} symmetry for the (CO)₆-Fe₂Ga₃ framework. The central part of the molecule can also be viewed as an Fe₂Ga₃ cluster of trigonal-bipyramidal symmetry with the iron atoms in axial and the gallium atoms in equatorial positions. The remaining six terminal carbonyl ligands are orientated in an eclipsed conformation in relation to the iron–iron vector. The Fe–Fe distance in **5** (2.908(6) Å) is elongated in comparison to Fe₂(CO)₉ (2.522(1) Å)²³ but shortened compared to the distance in (CO)₃Fe[μ -InC(SiMe₃)₃]₃-Fe(CO)₃ (2.992(2) Å).^{9a} The effect of different bridging units X in Fe₂(CO)₆(μ -X)₃ complexes on the respective

(20) Braga, D.; Grepioni, F.; Orpen, A. G. *Organometallics* **1993**, *12*, 1481.

(21) Pickardt, J.; Rösch, L.; Schumann, H. *J. Organomet. Chem.* **1976**, *107*, 241.

(22) Riley, P. E.; Davis, R. E. *Inorg. Chem.* **1980**, *19*, 159.

(23) Cotton, F. A.; Troup, J. M. *J. Chem. Soc., Dalton Trans.* **1974**, 800.



Fe–Fe distances has been discussed in more detail by Uhl et al.^{9a}

The structure-determining space requirement of the three gallium-bonded Cp* ligands prohibits a molecular C_{3v} symmetry with a C_3 axis along the Fe–Fe vector. Thus, deviations from the ideal η^5 -bonding within the Cp*–Ga units and from symmetrical μ_2 -coordination (equal Ga–Fe bonds) finally lead to only molecular mirror symmetry. In fact, the molecule is located on a crystallographic mirror plane. The most obvious deviation from η^5 -coordination is observed for the Cp* ligand at Ga(2). From the bond lengths and angles given in Table 5, one can conclude an η^3/η^1 coordination mode. Thus, the Ga(2)–C(11) bond length (2.087(7) Å) is in the range of Ga–C(Cp*) σ -bonds. For comparison, in Cp*GaX₂ compounds, the (Cp*)C–Ga distance is 2.008(6) Å for X = I and 1.97(1) Å for X = Cl.¹² Furthermore, the C(14) methyl group is bent away from the Cp ring plane by 17.7°, indicating a tendency for sp³-hybridization at carbon atom C(11). Much smaller deviations from ideal η^5 -coordination are observed for the remaining two Cp*Ga units (Ga(1)–Cp*; Ga(1a)–Cp*; see Table 5). The described deviations from ideal η^5 -Cp*–Ga bonding correspond to the observed asymmetry in the μ_2 -GaCp* bridging situations. As seen from Table 5, the Ga–Fe bond lengths vary between 2.354(4) and 2.454(3) Å.

The asymmetry observed for **5** in the solid state is not maintained in solution, where NMR spectroscopic data indicate dynamic processes, which finally lead to an averaged information on the basis of a molecular C_{3v} symmetry. Thus, the ¹H NMR spectrum of **5** shows only one sharp singlet at $\delta = 2.05$ ppm for the Cp* methyl groups, indicating only one type of Cp*Ga ligand. In agreement with this result, the ¹³C NMR spectrum shows one resonance for the Cp* methyl groups (δ 10.85 ppm) and one resonance for the Cp* ring carbon atoms (δ 119.21 ppm). Furthermore, one resonance for the six carbonyl carbon atoms is observed (δ 216.73 ppm). In the ν_{CO} region of the IR spectrum, only these absorptions are observed, which are in the typical range for terminal CO ligands (1951 and 1923 cm⁻¹). Due to its thermal stability, compound **5** can be characterized by standard EI-MS techniques. At a sample temperature of approximately 400 °C, a strong signal for the molecular ion is detected at 894 amu with the correct isotopic pattern. Successive loss of Cp*Ga and CO units is observed. The loss of one Cp*Ga and three CO ligands leads to a fragment at 606 amu with the highest intensity.

When Cp*Ga (**1**) was reacted with Co₂(CO)₈ in a *n*-hexane solution, rapid gas evolution occurred already at room-temperature, indicating substitution of carbon monoxide. Heating of the reaction mixture completed the formation of the compound (CO)₃Co[μ_2 -Ga(η^5 -Cp*)]₂Co(CO)₃ (**6**), which precipitated as an air-sensitive orange-red powder in good yield (see Scheme 5). Compound **6** is only poorly soluble in aprotic organic solvents. In the solid state, the complex decomposes at

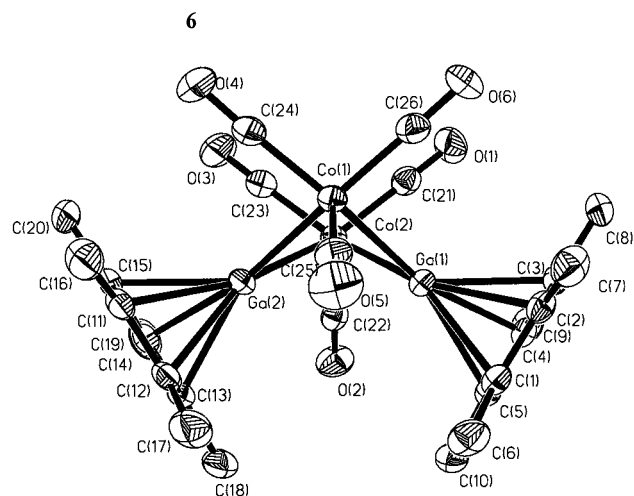


Figure 5. Molecular structure of (CO)₃Co[μ_2 -(η^5 -Cp*Ga)]₂-Co(CO)₃, **6**.

Table 6. Selected Bond Lengths (Å) and Angles (deg) for **6**

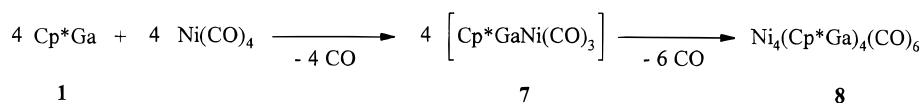
Ga(1)–C(1)	2.241(3)	Ga(2)–C(11)	2.289(3)
Ga(1)–C(2)	2.275(3)	Ga(2)–C(12)	2.261(3)
Ga(1)–C(3)	2.315(3)	Ga(2)–C(13)	2.264(3)
Ga(1)–C(4)	2.338(3)	Ga(2)–C(14)	2.303(3)
Ga(1)–C(5)	2.289(3)	Ga(2)–C(15)	2.295(3)
Ga(1)–Co(1)	2.3926(5)	Co(1)–Co(2)	2.8278(6)
Ga(1)–Co(2)	2.3784(5)	Co(2)–C(21)	1.778(4)
Ga(2)–Co(1)	2.3959(5)	Co(2)–C(22)	1.771(4)
Ga(2)–Co(2)	2.3884(5)	Co(2)–C(23)	1.777(3)
O(1)–C(21)	1.146(4)	Co(1)–C(24)	1.780(4)
O(2)–C(22)	1.145(4)	Co(1)–C(25)	1.769(4)
O(3)–C(23)	1.146(4)	Co(1)–C(26)	1.779(4)
O(4)–C(24)	1.141(4)		
O(5)–C(25)	1.146(4)		
O(6)–C(26)	1.139(4)		
Co(2)–Ga(1)–Co(1)	72.696(17)	C(25)–Co(1)–C(26)	109.15(16)
Co(2)–Ga(2)–Co(1)	72.461(17)	C(25)–Co(1)–C(24)	107.82(16)
Ga(1)–Co(1)–Co(2)	53.420(15)	C(26)–Co(1)–C(24)	99.74(15)
Ga(1)–Co(2)–Co(1)	53.883(14)	C(22)–Co(2)–C(21)	110.25(15)
Ga(2)–Co(2)–Co(1)	53.892(15)	C(22)–Co(2)–C(23)	108.01(15)
Ga(2)–Co(1)–Co(2)	53.647(14)	C(23)–Co(2)–C(21)	99.04(15)
O(1)–C(21)–Co(2)	178.1(3)	C(21)–Co(2)–Co(1)	97.96(11)
O(2)–C(22)–Co(2)	174.8(3)	C(22)–Co(2)–Co(1)	135.14(11)
O(3)–C(23)–Co(2)	176.5(3)	C(23)–Co(2)–Co(1)	100.82(11)
O(4)–C(24)–Co(1)	176.6(3)	C(24)–Co(1)–Co(2)	100.29(12)
O(5)–C(25)–Co(1)	172.4(3)	C(25)–Co(1)–Co(2)	136.18(11)
O(6)–C(26)–Co(1)	177.5(3)	C(26)–Co(1)–Co(2)	98.11(12)

230 °C. Compound **6** could be crystallized from hot toluene as red needles suitable for an X-ray structure analysis.

The molecular structure of **6** is shown in Figure 5. Crystallographic data are collected in Table 1, and selected bond lengths and angles are collected in Table 6.

Compound **6** can be described as a derivative of the dinuclear cobalt carbonyl complex Co₂(CO)₈ in its solid-state structure, in which the bridging carbonyl ligands are replaced by bridging Cp*Ga units. The six terminal carbonyl ligands are orientated in an eclipsed conformation in relation to the cobalt–cobalt vector. Due to the pseudo C_{2v} symmetry, the CO–Co–Co plane represents a mirror plane of the molecule; a C_2 axis bisects the Co–Co vector. The Co–Co distance in **6** (2.8278(6)

Scheme 6



Å) is elongated in comparison to $\text{Co}_2(\text{CO})_8$ (2.5301(8) and 2.5278(8) Å)²⁴ and also to $(\text{CO})_3\text{Co}[\mu\text{-InC}(\text{SiMe}_3)_3]_2\text{Co}(\text{CO})_3$ (2.8014(6) Å).^{9b} In both Cp^*Ga units, the η^5 -bonding mode is maintained. The gallium atoms are located in approximately the central position above the Cp^* ring systems; the respective Ga–C(Cp^*) distances only vary between 2.241(3) and 2.338(4) Å (see Table 6) with an average value of 2.287(3) Å. Furthermore, all methyl groups are located within the corresponding C_5 -ring planes.

Despite its poor solubility even in benzene- d_6 , **6** could be characterized by NMR techniques. The ^1H and ^{13}C NMR spectra confirm the solid-state structure to be present also in solution. As expected for $\eta^5\text{-Cp}^*$ units, only one type of methyl group and ring carbon atom is found in the ^1H NMR (δ 1.93 ppm) and ^{13}C NMR spectrum (δ 9.94 and 116.75 ppm). The resonance for the six carbonyl carbon atoms can be detected only after a 12 h acquisition time as a very small and broad signal (δ 206.00 ppm). In the ν_{CO} region, the IR spectrum of **6** shows absorptions in the typical range for terminal CO ligands (between 2023 and 1948 cm^{-1}). In the EI mass spectrum of **6**, the molecular ion and the fragments formed by successive loss of carbon monoxide are detected with very small intensities; the spectrum is dominated by the loss of CO and Cp^*Ga .

When a solution of Cp^*Ga in n -hexane was added dropwise to an excess of $\text{Ni}(\text{CO})_4$, immediate gas evolution indicated CO substitution and a highly unstable colorless intermediate (**7**) was formed. Further stirring or gentle heating caused further gas evolution and a color change to red, which intensified after removing all volatile components in vacuo. The remaining red crystalline solid was characterized as the cluster compound $\text{Ni}_4(\text{Cp}^*\text{Ga})_4(\text{CO})_6$ (**8**) (see Scheme 6). In the solid state, **8** decomposes at 180 °C. The air-sensitive complex readily dissolves in the usual organic solvents. Recrystallization from n -hexane/toluene at 4 °C gave red plates of **8** suitable for an X-ray structure analysis.

The unstable intermediate is presumably the mono-substitution product $\text{Ni}(\text{Cp}^*\text{Ga})(\text{CO})_3$ (**7**), as indicated in an independent experiment. Thus, equimolar quantities of the starting materials were reacted in benzene- d_6 solution and investigated spectroscopically. Only a complexed Cp^*Ga unit was detected in the ^1H and ^{13}C NMR spectrum (^1H NMR 1.79 ppm ($\text{Cp}^*\text{-Me}$); ^{13}C NMR 9.94 ($\text{Cp}^*\text{-CH}_3$), 114.12 ppm (ring C)). The ^{13}C NMR spectrum showed an additional resonance at 196.81 ppm (CO). The IR spectrum in the carbonyl region showed two absorptions at 2066 (A_1) and 1996 cm^{-1} (E), as expected for a $\text{Ni}(\text{CO})_3\text{L}$ complex with a local C_{3v} symmetry. Compound **7** could not be isolated and turned out to be unstable under ordinary conditions (easy loss of CO and formation of **8**, see Scheme 6).

Compound **8** crystallizes with two molecules of toluene per formula unit. The molecular structure of **8** is depicted in Figure 6. Crystal structure parameters are

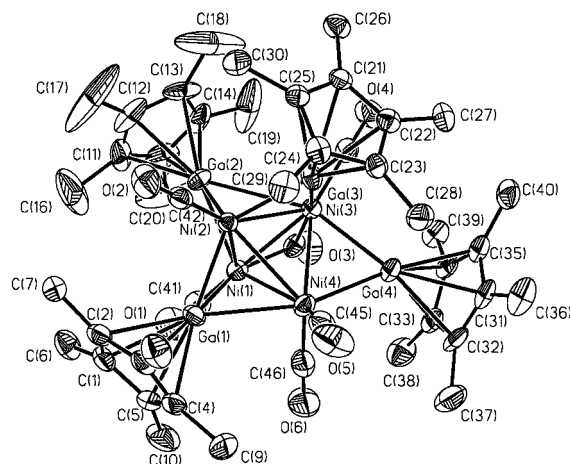


Figure 6. Molecular structure of $\text{Ni}_4(\text{Cp}^*\text{Ga})_4(\text{CO})_6$, **8**.

Table 7. Selected Bond Lengths (Å) and Angles (deg) for **8**

Ga(1)–Ni(1)	2.4599(13)	Ni(1)–C(43)	1.885(6)
Ga(1)–Ni(2)	2.3166(11)	Ni(1)–C(41)	1.729(6)
Ga(1)–Ni(4)	2.5824(12)	Ni(2)–C(42)	1.735(6)
Ga(2)–Ni(1)	2.4256(12)	Ni(3)–C(43)	1.942(6)
Ga(2)–Ni(2)	2.3173(13)	Ni(3)–C(44)	1.748(6)
Ga(2)–Ni(3)	2.8321(13)	Ni(4)–C(45)	1.754(6)
Ga(3)–Ni(2)	2.2933(11)	Ni(4)–C(46)	1.770(7)
Ga(3)–Ni(3)	2.4399(12)	O(1)–C(41)	1.153(7)
Ga(4)–Ni(3)	2.4452(12)	O(2)–C(42)	1.145(7)
Ga(4)–Ni(4)	2.4358(12)	O(3)–C(43)	1.161(7)
Ni(1)–Ni(2)	2.5080(12)	O(4)–C(44)	1.139(7)
Ni(1)–Ni(3)	2.4273(12)	O(5)–C(45)	1.142(7)
Ni(1)–Ni(4)	2.621(2)	O(6)–C(46)	1.153(8)
Ni(2)–Ni(3)	2.5926(13)		
Ni(2)–Ni(4)	2.6586(13)		
Ni(3)–Ni(4)	2.6579(13)		
Ni(1)–Ni(3)–Ni(2)	59.84(3)	Ni(2)–Ni(1)–Ni(4)	62.40(4)
Ni(1)–Ni(4)–Ni(2)	56.72(3)	Ni(3)–Ni(1)–Ni(4)	63.40(4)
Ni(1)–Ni(4)–Ni(3)	54.74(3)	Ni(3)–Ni(2)–Ni(4)	60.80(4)
Ni(1)–Ni(2)–Ni(4)	60.89(4)	Ni(3)–Ni(4)–Ni(2)	58.37(4)
Ni(2)–Ni(3)–Ni(4)	60.83(4)		

given in Table 1, and selected bond lengths and angles are collected in Table 7.

Compound **8** possesses a Ni_4 tetrahedron as its central framework. The Ni_4 tetrahedron is strongly distorted, and the Ni–Ni distances vary from 2.4273(12) to 2.6586(13) Å. Each Ni atom is coordinated by a terminal CO ligand. Additionally, one of the remaining CO ligands coordinates terminally to a Ni atom (Ni(4)) while the other is in a bridging position (between Ni(1) and Ni(3)). All C–O and Ni–C distances are in the expected range. Interestingly, the four Cp^*Ga ligands coordinate to the Ni core in a different manner. This is illustrated in Figure 7, which shows the orientation of the four gallium centers with respect to the Ni_4 tetrahedron. The coordination changes from a rather symmetrical μ_3 mode (gallium atom Ga(1)) to a μ_2 situation (gallium atom Ga(4)). The gallium atoms Ga(2) and Ga(3) coordinate to the Ni core in modes between symmetrical μ_2 or μ_3 situations. A terminal μ_1 coordination is not observed. As a consequence of the described bonding situation, the gallium–nickel distances are quite different, varying

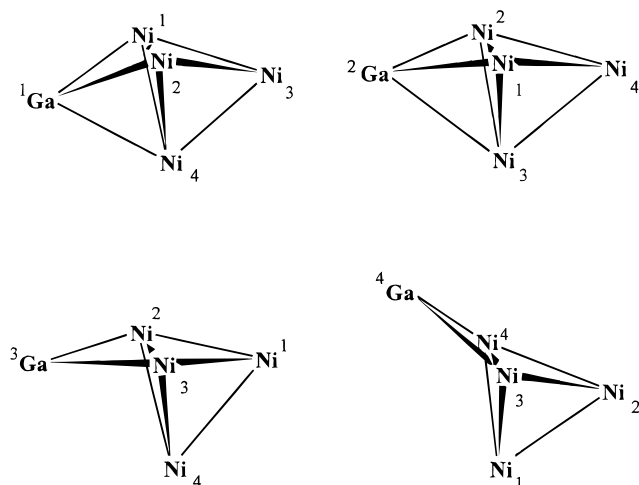


Figure 7. Coordination modes of Cp*Ga units in **8**. from 2.2933(11) to 2.8321(13) Å; the Ga(2)–Ni(3) bond is by far the longest (2.8321(13) Å); the average Ga–Ni distance is 2.455(1) Å. In all four Cp*Ga ligands, the η^5 coordination mode of the Cp* unit is maintained. Thus, the gallium atoms are located in approximately a central position above the Cp* ring planes; the average (Cp*)C–Ga distance is 2.322(6) Å. In addition, all methyl groups are in a plane with the corresponding C₅-ring perimeter. As a consequence of its molecular asymmetry, compound **8** crystallizes in space group $P\bar{1}$ in the form of enantiomers.

Lack of symmetry is also evident from the complexity of the band pattern in the IR spectrum. In the ν_{CO} region, four absorptions are observed both in the solid state and in solution. An absorption at 1830 cm^{-1} indicates the presence of bridging CO groups, whereas the other three absorptions at 2000, 1972, and 1950 cm^{-1} are typical for terminal CO ligands. In contrast, the ^1H and ^{13}C NMR measurements in solution indicate a highly fluxional structure of **8** on the NMR time scale. The ^1H NMR spectrum shows only one singlet at 2.02 ppm for the Cp* methyl groups. Correspondingly, the ^{13}C NMR spectrum shows one resonance for the Cp* methyl groups (10.18 ppm) and one resonance for the Cp* ring carbon atoms (115.38 ppm). In addition, only one resonance for the six carbonyl C atoms is observed at 208.58 ppm. Compound **8** decomposes at 180 °C. In EI-MS experiments, no nickel-containing fragments were observed; only the loss of Cp*Ga and CO was detected during heating, indicating decomposition under these conditions also.

Isoelectronic compounds of the type $\text{Ni}_4(\text{CO})_6\text{L}_4$ with $\text{L} = \text{PMe}_3$,²⁵ P^nBu_3 ,²⁵ and $\text{P}(\text{C}_2\text{H}_4\text{CN})_3$ ²⁶ are already known in the literature. In these compounds, the ligands L are in terminal and the CO ligands in bridging positions, leading to a skeletal T_d symmetry. A quite different situation is found in **8**, in which the ligands L (Cp*Ga) occupy bridging positions and the CO ligands are in terminal as well as in bridging positions.

Conclusions

A new method for the synthesis of pentamethylcyclopentadienylgallium, Cp*Ga (**1**), has been developed. The

(25) Bochmann, M.; Hawkins, I.; Yellowless, L. J.; Hursthouse, M. B.; Short, R. L. *Polyhedron* **1989**, *8*, 1351.

(26) Bennett, M. J.; Cotton, F. A.; Winqvist, B. H. C. *J. Am. Chem. Soc.* **1967**, *89*, 5366.

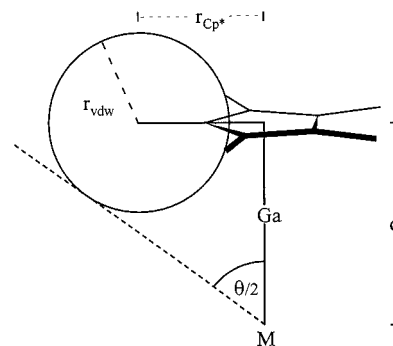


Figure 8. Determination of the cone angle of Cp*Ga in complexes. θ can be calculated by the following equation: $\tan \theta/2 = (d \times r_{\text{Cp}^*} + r_{\text{vdw}} \sqrt{d^2 + r_{\text{Cp}^*}^2 - r_{\text{vdw}}^2}) / d^2 - r_{\text{vdw}}^2$, where r_{vdw} = van der Waals radius of a methyl group; r_{Cp^*} = (Cp*)centroid – C(methyl) distance; d = (Cp*)centroid – M distance.

reductive dehalogenation of (pentamethylcyclopentadienyl)diiodogallane, Cp*GaI₂, leads to **1** in high yield, making it available in large-scale quantities. The exceptional thermal stability of **1** is noteworthy.

Due to the gallium-centered lone pair, **1** can act as a ligand in transition metal chemistry, replacing, for example, carbon monoxide or other weakly bound ligands. The first examples with **1** as a ligand are presented from the chemistry of chromium, iron, cobalt, and nickel. They show that **1** can bind in terminal as well as in bridging positions. Connection to two (μ_2) or even three (μ_3) metal centers in a more or less symmetrical arrangement as in **5**, **6**, and **8** characterizes the bridging situation. A terminal position is restricted to mononuclear complexes such as **3**, **4**, and **7**.

It is interesting to note that π -bonding between the Cp* unit and the gallium atom is preserved in all transition metal complexes synthesized so far. An η^5 -coordination is generally observed; but steric congestion can lead to an η^3/η^1 bonding mode, as documented in one of the three Cp*Ga ligands in the solid-state structure of complex **5**. Remember that haptotropic shifts can easily occur in Cp compounds of the main group elements.¹⁰ The spacial requirements of an η^5 -Cp*Ga ligand is documented by its cone angle, θ ,²⁷ which can be determined using simple trigonometric calculations. Thus, with the van der Waals radius of a methyl group (2.00 Å),²⁸ with the average (Cp*)centroid–C(Me) distance (2.717 Å) and with an averaged (Cp*)centroid–M distance (4.226 Å, taken from the structural data of **3** and **4**), one can calculate a cone angle of 112°, as shown in Figure 8. For comparison, the cone angle of PF₃, PH₂Et, PMe₃, PET₃, and PPh₃ is 104°, 111°, 118°, 132°, and 145°, respectively.²⁹

In transition metal chemistry, common ligands are characterized with respect to their σ -donor/ π -acceptor properties. A corresponding classification of the Cp*Ga ligand can be performed on the basis of X-ray crystal structural data (Cp*–Ga and M–CO distances) and on the basis of IR data (ν_{CO} region, trans effect). Crystal structure data of **3** and **4** show that the (Cp*)C–Ga bonds are shortened by approximately 7% in comparison

(27) Tolman, C. A. *Chem. Rev. (Washington, D.C.)* **1977**, *77*, 313.

(28) Pauling, L. *Die Natur der chemischen Bindung*, zweite Aufl.; Verlag Chemie: Weinheim, 1964; p 245.

(29) White, D.; Coville, N. J. *Adv. Organomet. Chem.* **1994**, *36*, 95.

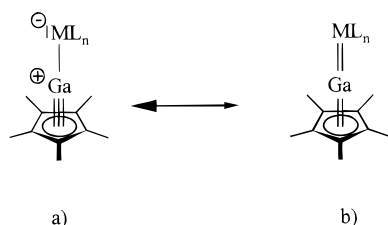


Figure 9. Resonance structures of Cp^*GaML_n complexes.

to those of Cp^*Ga in the solid state³ or in the gas phase.⁴ Reduced distances indicate stronger σ -bonding due to the presence of a gallium atom in a comparatively higher oxidation state and allow the Cp^*Ga ligand to be classified as a predominant σ -donor in a strongly polarized bond ($\text{Ga}^{\delta+}-\text{M}^{\delta-}$). The converse effect (predominant π -acceptor) should result in longer (Cp^*)C–Ga distances and possibly in a change in hapticity from η^5 to η^3 or even η^1 ; this phenomenon is not observed.

Predominant σ -donor behavior of the Cp^*Ga ligand should also result in a strengthening of the transoid metal–carbon bond and in a weakening of the respective carbon–oxygen bond (trans effect). As expected, shorter trans M–CO bonds are observed in the structures of **3** and **4**, compared to the situation in the binary carbonyl complexes $\text{Cr}(\text{CO})_6$ and $\text{Fe}(\text{CO})_5$. Details have been discussed earlier.

In compounds of the type $\text{LCr}(\text{CO})_5$, $\text{LFe}(\text{CO})_4$, and $\text{LNi}(\text{CO})_3$, the ν_{CO} symmetric stretching band ($A_1(1)$ or A_1) strongly depends on the trans-positioned ligand L. For comparison, complexes with $L = \text{PR}_3$ and Cp^*Ga are considered in more detail. Thus, in $\text{LCr}(\text{CO})_5$ complexes, the $A_1(1)$ mode is observed at 1943 ($L = \text{PEt}_3$),³⁰ 1942 ($L = \text{PPh}_3$)³¹, and 1918 cm^{-1} ($L = \text{Cp}^*\text{Ga}$); in $\text{LFe}(\text{CO})_4$ complexes, the $A_1(1)$ mode is found at 1966 ($L = \text{PEt}_3$),³² 1977 ($L = \text{PPh}_3$),³³ and 1966 cm^{-1} ($L = \text{Cp}^*\text{Ga}$); finally, in $\text{LNi}(\text{CO})_3$ complexes, the A_1 mode is observed at 2061 ($L = \text{PEt}_3$),³⁴ 2068 ($L = \text{PPh}_3$),³⁴ and 2066 cm^{-1} ($L = \text{Cp}^*\text{Ga}$). An inspection of those data without recourse to force constants shows that the ligand Cp^*Ga is similar in its electronic properties to triorganophosphanes, which are regarded as strong donors but poor acceptors.³⁵

In a valence-bond picture, the predominant σ -donor ability of the Cp^*Ga ligand is best represented by resonance structure a in Figure 9. A comparable bonding situation has been described for $\text{Fe}(\text{Cp}^*\text{Al})(\text{CO})_4$ on the basis of crystal structure and spectroscopic data and DFT calculations for the parent complex, $\text{Fe}(\text{CpAl})(\text{CO})_4$, only recently by Fischer et al.^{8b} In comparison to the Cp^*Ga ligand, the σ -donor properties of anionic R_2Ga^- and of donor-stabilized RGA ligands are even more predominant, as also reported by Fischer et al.^{36,37}

The easy availability of Cp^*Ga should allow the synthesis of further transition metal complexes with

(30) Dalton, J.; Paul, I.; Smith, J. G.; Stone, F. G. A. *J. Chem. Soc. A* **1968**, 1195.

(31) Delbecke, F. T.; van der Kelen, G. P. *J. Organomet. Chem.* **1974**, *64*, 239.

(32) Inoue, H.; Nakagome, T.; Kuroiwa, T.; Shirai, T.; Fluck, E. Z. *Naturforsch. B* **1987**, *42*, 573.

(33) Darenbourg, D. J.; Nelson, H. H. III; Hyde, C. L. *Inorg. Chem.* **1974**, *13*, 2135.

(34) Tolman, C. A. *J. Am. Chem. Soc.* **1970**, *92*, 2953.

(35) Bochmann, M. *Organometallics I*; Oxford University Press: London, 1994; p 14.

(36) Fischer, R. A.; Schulte, M. M.; Herdtweck, E.; Mattner, M. R. *Inorg. Chem.* **1997**, *36*, 2010.

this novel ligand. Interesting chemical properties of the new complexes can be envisaged due to the flexibility in Cp^* bonding ($\eta^5-\eta^3-\eta^1$) and due to the leaving-group character of the Cp^* unit.

Experimental Section

General Data. All manipulations were carried out under a purified argon atmosphere using standard vacuum techniques. The solvents were commercially available, purified by conventional means, and distilled immediately prior to use. The ultrasonic metal activation was performed using a Bioblock Scientific Vibra-Cell (72412) apparatus. GaI_3 was prepared from the elements and sublimed in vacuo. $\text{Fe}_2(\text{CO})_9$, $\text{Co}_2(\text{CO})_8$, and $\text{Ni}(\text{CO})_4$ were commercially available and used without further purification. $\text{Cr}(\text{CO})_5(\text{C}_8\text{H}_{14})$,¹⁶ $\text{Fe}(\text{CO})_3\text{CHT}$,³⁸ and Cp^*SiMe_3 ¹¹ can be prepared according to the literature. The melting point determinations were performed using a Büchi 510 melting point apparatus. Elemental analyses were performed by the Microanalytical Laboratory of the Universität Bielefeld. The NMR spectra were recorded in benzene- d_6 using a Bruker Avance DRX 500 spectrometer (^1H 500.1 MHz; $^{13}\text{C}\{^1\text{H}\}$ 125.8 MHz). Chemical shifts are reported in ppm and are referenced to benzene as an internal standard. IR data were collected using a Bruker Vektor 22-FT spectrometer. The samples were measured as KBr pellets or in solution between KBr windows. Absorption intensities are reported with abbreviations w (weak), m (medium), s (strong), vs (very strong), and sh (shoulder). Mass spectrometry was performed using a VG Autospec spectrometer. Only characteristic fragments and isotopes of the highest abundance are listed.

Preparation of Cp^*GaI_2 (2**).** A solution of Cp^*SiMe_3 (2.51 g, 12.0 mmol) in *n*-hexane (15 mL) was added dropwise to a refluxing suspension of GaI_3 (5.41 g, 12.0 mmol) in *n*-hexane (35 mL). While the reaction mixture was heated at reflux for 1 h, the color changed to red. Apart from a small amount of solid decomposition products, all components were soluble. After separation of the solution, all volatile components were removed in vacuo. The remaining solid was recrystallized from a *n*-hexane (50 mL)/toluene (10 mL) mixture to give 4.91 g (10.7 mmol) of Cp^*GaI_2 , **2** (89% yield).

Decomposition point: 122°C . ^1H NMR: $\delta = 1.71$ (s, 15 H, Cp^* methyl). ^{13}C NMR: $\delta = 11.69$ (Cp^* methyl), 122.28 (Cp^* ring). MS (EI, 70 eV) [m/z (rel int.)]: 450 [GaI_3^+ (49)], 323 [GaI_2^+ (89)], 136 [Cp^*H^+ (50)], 127 [I^+ (66)], 121 [$\text{Cp}^*\text{H}^+ - \text{CH}_3$ (100)]. Anal. Calcd for $\text{C}_{10}\text{H}_{15}\text{GaI}_2$ ($M = 458.76 \text{ g mol}^{-1}$): C, 26.18; H, 3.29. Found: C, 25.8; H, 3.26.

Preparation of Cp^*Ga (1**).** Potassium, 0.98 g (10.0 mmol), was added to a solution of 4.59 g (10.0 mmol) of Cp^*GaI_2 (**2**) in 40 mL of toluene. During sonification with 200 W for 10 min, the reaction mixture was allowed to warm to 70°C to melt the potassium metal. After filtration and extraction of the remaining grayish solid with 20 mL of toluene, the solvent was removed from the combined yellow solutions. The remaining oil was distilled at 80°C (8 Torr) to give 1.43 g (7.0 mmol) of Cp^*Ga (**1**) (70% yield) as a light yellow liquid, which solidified after several days during storage at 4°C .

^1H NMR: δ 1.92 (s, 15 H, Cp^* methyl). ^{13}C NMR: δ 10.06 (Cp^* methyl), 113.51 (Cp^* ring).

Preparation of $\text{Cr}(\text{Cp}^*\text{Ga})(\text{CO})_5$ (3**).** A solution of $(\text{C}_8\text{H}_{14})\text{Cr}(\text{CO})_5$ (0.40 g, 1.32 mmol) and Cp^*Ga (**1**) (0.29 g, 1.41 mmol) in 12 mL of *n*-hexane was refluxed for 1 h. On cooling to room temperature, the product precipitated as a yellow powder. Subsequently, all volatile components were removed in vacuo to yield 0.45 g (1.13 mmol; 86%) of $\text{Cr}(\text{Cp}^*\text{Ga})(\text{CO})_5$ (**3**).

(37) Schulte, M. M.; Herdtweck, E.; Raudaschl-Sieber, G.; Fischer, R. A. *Angew. Chem.* **1996**, *108*, 489; *Angew. Chem., Int. Ed. Engl.* **1996**, *35*, 424.

(38) Brauer, G. *Handbuch der Präparativen Anorganischen Chemie* i 3 Bd. Stuttgart Enke 1981; p 1891.

Mp: 156 °C. ¹H NMR: δ 1.64 (s, 15 H, Cp* methyl). ¹³C NMR: δ 8.86 (Cp* methyl), 115.20 (Cp* ring), 219.01 (CO_{equatorial}), 224.26 (CO_{axial}). IR (cm⁻¹, KBr): 2052 (s, ν_{CO}, A₁(2)), 1982 (s, ν_{CO}, B₁), 1918 (vs, ν_{CO}, A₁(1)), 1902 (vs, ν_{CO}, E), 1390 (w), 675 (m), 654 (s), 473 (w). MS (EI, 70 eV) [*m/z* (rel int.)]: 396 [M⁺ (9)], 340 [M⁺ - 2CO (3)], 312 [M⁺ - 3CO (5)], 284 [M⁺ - 4CO (5)], 256 [M⁺ - 5CO (100)], 204 [Cp*Ga⁺ (10)], 136 [Cp*⁺ (19)], 119 [CpH⁺ - CH₃(22)], 69 [Ga (29)]. Anal. Calcd for C₁₅H₁₅O₅CrGa (*M* = 396.99 g mol⁻¹): C, 45.38; H, 3.81. Found: C, 45.34; H, 3.80.

Preparation of Fe(Cp*Ga)(CO)₄ (4). A suspension of Fe₂(CO)₉ (1.82 g; 5.00 mmol) and Cp*Ga (1) (1.02 g; 5.00 mmol) in 30 mL of *n*-hexane was stirred at room temperature with exclusion of light for 48 h. Subsequently, all volatile components were removed in vacuo from the black solution. The residual black solid was extracted with 30 mL of hot *n*-hexane. The solution was cooled to -60 °C to crystallize the crude product. Recrystallization from *n*-hexane yielded 0.53 g (1.42 mmol; 28%) of Fe(Cp*Ga)(CO)₄ (4) as a yellow solid.

Decomposition point: 112 °C. ¹H NMR: δ = 1.60 (s, 15 H, Cp* methyl). ¹³C NMR: δ 8.77 (Cp* methyl), 115.43 (Cp* ring), 214.21 (CO). IR (cm⁻¹, *n*-hexane; ν_{CO}): 2037 (s, ν_{CO}, A₁(2)), 1966 (s, ν_{CO}, A₁(1)), 1942 (vs, ν_{CO}, E). MS (EI, 70 eV) [*m/z* (rel int.)]: 372 [M⁺ (7)], 344 [M⁺ - CO (11)], 316 [M⁺ - 2CO (24)], 288 [M⁺ - 3CO (11)], 260 [M⁺ - 4CO (100)], 204 [Cp*Ga⁺ (28)], 134 [Cp*⁺ (7)], 119 [Cp*⁺ - CH₃ (20)], 69 [Ga⁺ (50)]. Anal. Calcd for C₁₄H₁₅O₄FeGa (*M* = 372.84 g mol⁻¹): C, 45.10; H, 4.06. Found: C, 45.03; H, 4.06.

Preparation of Fe₂(Cp*Ga)₃(CO)₆ (5). A solution of Cp*Ga (1) (0.73 g, 3.56 mmol) in toluene (2 mL) was added dropwise to a solution of Fe(CO)₃CHT (0.55 g, 2.37 mmol) in toluene (5 mL). While the reaction mixture was heated at reflux for 1 h, the color of the solution changed to red. After the mixture was cooled to room temperature, all volatile components were removed in vacuo to yield 0.63 g of Fe₂(Cp*Ga)₃(CO)₆ (0.70 mmol, 59%).

Decomposition point: 270 °C. ¹H NMR: δ 2.05 (s, 15 H, Cp* methyl). ¹³C NMR: δ 10.85 (Cp* methyl), 119.21 (Cp* ring), 216.73 (CO). IR (cm⁻¹; KBr): 2912 (m, sh), 2861 (m), 1951 (vs, sh), 1923 (vs), 1447 (m), 1379 (m), 1028 (w), 585 (s). MS (EI, 70 eV) [*m/z* (rel int.)]: 894 [M⁺ (21)], 782 [M⁺ - 4CO (3)], 606 [M⁺ - 3CO - Cp*Ga (100)], 494 [M⁺ - 5CO - Fe - Cp*Ga (27)], 204 [Cp*Ga⁺ (19)], 135 [Cp*⁺ (6)], 119 [Cp*⁺ - CH₃ (16)], 69 [Ga⁺ (36)]. Anal. Calcd for C₃₆H₄₅O₆Fe₂Ga₃ (*M* = 894.61 g mol⁻¹): C, 48.33; H, 5.07. Found: C, 48.08; H, 5.09.

Preparation of Co₂(Cp*Ga)₂(CO)₆ (6). Cp*Ga (1) (1.07 g, 5.22 mmol) in *n*-hexane (5 mL) was added dropwise to a solution of Co₂(CO)₈ (0.89 g, 2.61 mmol) in *n*-hexane (15 mL),

whereupon immediate gas evolution was observed. While the solution was heated at reflux for 30 min, the product precipitated as an orange powder. After removal of all volatile components in vacuo, the brown-red residue was washed with 10 mL of *n*-hexane to yield 0.76 g (1.04 mmol, 42%) of Co₂(Cp*Ga)₂(CO)₆.

Decomposition point: 230 °C. ¹H NMR: δ 1.93 (s, 15 H, Cp* methyl). ¹³C NMR: δ 9.94 (Cp* methyl), 116.75 (Cp* ring), 206.00 (wide, CO). IR (cm⁻¹, KBr): 2920 (m, sh), 2863 (m), 2023 (s), 1989 (s), 1953 (vs), 1948 (vs, sh), 1640 (w), 1449 (w), 1416 (w), 1383 (m), 550 (m), 522 (m), 501 (w), 470 (w). MS (EI, 70 eV) [*m/z* (rel int.)]: 696 [M⁺ (<0.1)], 668 [M⁺ - CO(1)], 640 [M⁺ - 2CO(1)], 584 [M⁺ - 4CO(1)], 556 [M⁺ - 5CO(0.1)], 526 [overlapping of M⁺ - 6CO and M⁺ - 4CO - CO (3)], 204 [Cp*Ga⁺ (95)], 135 [Cp*⁺ (11)], 119 [Cp*⁺ - CH₃ (32)], 69 [Ga⁺ (91)]. Anal. Calcd for C₂₆H₃₀O₆Co₂Ga₂ (*M* = 695.83 g mol⁻¹): C, 44.88; H, 4.35. Found: C, 44.89; H, 4.31.

Preparation of Ni₄(Cp*Ga)₄(CO)₆ (8). Cp*Ga (1) (0.74 g, 3.61 mmol) in *n*-hexane (5 mL) was added dropwise with stirring to an excess of neat Ni(CO)₄ (10.00 g, 58.6 mmol). Immediate gas evolution was observed, and the solution remained colorless. During stirring and gentle heating, further gas evolution occurred, whereupon the color changed to red. The color intensified when all volatile components were removed in vacuo, giving **8** as a red crystalline solid (1.00 g, 0.82 mmol, 91% yield based on Cp*Ga).

Decomposition point: 180 °C. ¹H NMR: δ 2.02 (s, 15 H, Cp* methyl). ¹³C NMR: δ 10.18 (Cp* methyl), 115.38 (Cp* ring), 208.58 (CO). IR (cm⁻¹, KBr): 2976 (w), 2912 (m), 2858 (m), 2000 (s), 1972 (vs), 1950 (vs), 1834 (m), 1444 (w), 1419 (w), 1377 (m); C₆H₆ solution (CO range): 2001 (s), 1973 (vs), 1951 (vs), 1826 (m). MS (EI, 70 eV) [*m/z* (rel int.)]: 204 [Cp*Ga⁺ (24)], 136 [Cp*H⁺ (32)], 134 [Cp*⁺ - H (32)], 121 [Cp*H⁺ - CH₃ (60)], 119 [Cp*⁺ - H - CH₃ (100)]. Anal. Calcd for C₄₆H₆₀O₆Ni₄Ga₄ (*M* = 1222.69 g mol⁻¹): C, 45.19; H, 4.95. Found: C, 44.75; H, 4.68.

Acknowledgment. The support of this work by the Deutsche Forschungsgemeinschaft, the Universität Bielefeld, and the Fond der Chemischen Industrie is gratefully acknowledged. We thank T. Pott for excellent preparative work.

Supporting Information Available: Tables of crystal data, positional and thermal parameters, and selected bond lengths and angles (44 pages). Ordering information is given on any current masthead page.

OM970913A